Investigating the Interaction of Water Vapour with Aminopropyl Groups on the Surface of Mesoporous Silica Nanoparticles

UNIVERSITÀ DEGLI STUDI DI TORINO

Investigating the interaction of water vapour with aminopropyl groups on the surface of mesoporous silica nanoparticles

G. Paul,[a] G. E. Musso,[b] E. Bottinelli,[b] M. Cossi,[a] L. Marchese,[a] and G. Berlier[b]*

[a] Dipartimento di Scienze e Innovazione Tecnologica and Centro Nano-SiSTeMI, Università del Piemonte Orientale, A. Avogadro, Via T. Michel 11 - 15121 Alessandria, Italy [b] Università di Torino, Department of Chemistry and NIS Centre, Via P. Giuria 7, 10125 Torino, Italy

Abstract

The interaction of water molecules with the surface of hybrid silica based mesoporous materials is studied by ^{29}Si, ^{1}H, ^{13}C Solid State Nuclear Magnetic Resonance (SS NMR) and infrared spectroscopy, and supported by ab initio calculations. The surface of aminopropyl grafted mesoporous silica nanoparticles (NH_2-MSN) was studied in the dehydrated state and upon interaction with controlled doses of water vapour. Former investigations described the interactions between aminopropyl and residual Si-OH groups: the present study shows the presence of hydrogen bonded species (Si-OH to NH_2) and weakly interacting "free" aminopropyl chains with a restricted mobility, together with a small amount of protonated NH_3^+ groups. The concentration of the latter species increased upon water interaction, indicating a reversible and fast proton exchange from water molecules to a fraction of the amino groups. Here this is discussed and explained for the first time, with a combined experimental and theoretical approach.

Introduction

The importance of organic-inorganic hybrid silica-based materials in many fields of chemistry and related areas such as electrochemistry,[1-5] catalysis,[6-14] separation,[12, 15] adsorption,[16, 17] CO_2 capture[16, 18, 19] or nanomedicine[20-24] has steadily increased in recent years. Particular attention has been focused on ordered mesoporous silicas (OMS), thanks to the intrinsic high surface area, ordered and tuneable pore array with controlled size and huge available volume to host, react and release molecules, coupled to the ease of surface functionalization.[6, 20, 22, 25, 26] Mesoporous silica nanoparticles (MSN) are a class of OMS particularly important in the field of nanomedicine. They can be exploited as 'nanocarriers' for drug delivery applications, and even coupled to agents for diagnostics to obtain 'pharmaceutically adapted platforms'.[22, 27]

In the various applications listed above, the aminopropyl functional group plays an important role.[19, 28-34] This can be obtained from organosilanes differing from the terminating alkoxy groups, namely as 3-aminopropyl triethoxysilane (APTS, the most commonly employed), 3-aminopropyl methyldiethoxysilane or 3-aminopropyl dimethylethoxysilane.[35-39] Many other silica materials functionalized with amino-bearing functional groups have been studies, such as N-[N-(2-aminoethyl)-2-aminoethyl]-3-aminoproyl, N-(2-aminoethyl)-3-aminopropyl,[40] N-(2-aminoethyl)-3-aminoisobuthyldimethyl, 4-aminobutyl,[29] multiarm cyclam groups,[41] or hyperbranched poly(ethyleneimine).[42] This functionalization is usually aimed at optimizing the interaction with the desired target adsorptive: CO_2 in carbon Capture and Storage (CCS) applications, pollutants in environmental applications, reactants in catalysis, drugs in nanomedicine, etc. Moreover, surface functionalization can severely influence important material properties such as surface charge,[32, 34, 42] hydrophilicity,[34, 43, 44] dispersibility,[22] toxicity,[45] stability,[30, 41] etc.

The surface chemistry of amino-functionalized silica materials can be quite complex, as a result of the interactions between amino and silanol groups, resulting in a variety of hydrogen-bonded

structures and in the formation of NH_3^+/SiO^- couples.[28, 32, 33, 40, 46, 47] Moreover, Blitz et al. recently showed that surface amino groups can have a catalytic effect on the reactivity of vicinal silanols.[29] This complexity is influenced by the surrounding environment, and water is clearly the most common and important medium (or contaminant, when present as water vapour) for many applications. Indeed, many interesting works have been reported about the reactivity and stability of aminopropyl-grafted silica in water.[28, 30, 31, 33, 34, 39, 41, 46]

The influence of the amino groups on the acid-base properties of silica has been the subject of recent studies, mainly focused on their pH response in solutions. Walcarius et al. studied the acid-base equilibria taking place between aminopropyl and vicinal silanol groups, resulting in NH_3^+/SiO^- couples,[33, 46] while Etienne et al. pointed out that proton transfer at the silica surface with corresponding amine protonation could seriously affect the stability of this material in aqueous environment.[30] On the other hand, the protonation of the amino groups as a function of pH was studied with different techniques, including XPS and high resolution NMR in solution.[31, 39] Calvo et al. showed the influence of the chemical composition of inorganic mesoporous thin films on the pKa of surface aminoproyl groups, and supported their results with DFT molecular modelling.[28] Lehman et al. studied the chemical changes taking place at the liquid-solid interface, with focus on surface ligands stability and dynamics, by employing advanced NMR techniques.[31] These studies point to the importance of a detailed characterization of surface ligands, particularly when the materials are implemented in biomedical and environmental applications.[28, 31]

In this work, the surface of aminopropyl functionalized silica mesoporous nanoparticles (hereafter NH_2-MSN), is characterized by coupling Solid State NMR (SS NMR), Fourier Transform Infrared (FTIR) spectroscopies in controlled atmosphere and DFT molecular modelling. These techniques are applied to the material treated in vacuum and subsequently contacted with very small amounts of water vapour, to follow the interaction of water molecules with surface groups. The dynamics of water molecules localized to the functionalized silica

surface is experimentally measured by ^{1}H, ^{13}C and ^{29}Si SS NMR spectroscopy,[48] while the perturbation of the vibrational modes of aminoproyl and silanol groups upon water interaction is followed by FTIR. Both techniques point to the presence of a consistent proton transfer to a fraction of the amino groups in the presence of few adsorbed water molecules. This results is particularly important since it clearly shows that aminoproyl protonation can take place even in presence of water moisture, which could affect the long-term stability of the material. DFT molecular modelling is employed to interpret the results and give a realistic picture of the surface of this important class of hybrid materials. Results suggest that this peculiar reactivity towards few water molecules could be related to the mesoporous structure of the material, resulting in curved surfaces and/or relatively high concentration of surface groups and water molecules at the pores entrance.

2. Experimental section

All reactants and solvents were purchased from Sigma-Aldrich and employed as received. MSN sample was prepared by using cetyltrimethylammonium bromide (CTAB) as structure directing agent (SDA) according to a slightly modified literature procedure.[49, 50] NH_2-MSN sample was prepared with 3-aminopropyl triethoxysilane (APTS) by post-synthesis grafting with a procedure modified from the literature.[51, 52] Namely, 1 g of MSN (overnight dried at 100°C) were suspended in 30 ml of anhydrous toluene. The particles suspension was heated at 130°C under stirring. Next, 0.6 ml of APTS were added drop-wise and the mixture was allowed to reflux for 17 h. The modified amino-MSNs were filtered off and washed with toluene, ethanol, deionized water and at last methanol. Subsequently the sample was dried at 110°C for 3 h to favor the curing [36] and at 80°C overnight.

High Resolution Transmission Electron Microscopy (HRTEM) analyses were performed by means of a JEM 3010-UHR microscope (JEOL Ltd.) operating at 300 kV. For the measurements, MSN and NH_2-MSN powders were dispersed on a copper grid coated with a perforated carbon film. The size

distribution of the samples was obtained by measuring a statistically representative number of particles (*ca.* 200 particles) and the results are indicated as mean particle diameter (dm) ± standard deviation (STD) (dm±STD).

Specific surface area (SSA), cumulative pore volume and pore size distribution of samples overnight outgassed at room temperature (RT) were measured by N_2 adsorption-desorption isotherms at liquid nitrogen temperature (LNT) using a ASAP 2020 physisorption analyser (Micromeritics). The SSA was calculated by the Brunauer-Emmett-Teller (BET) method and the average pore size was determined by means of the Barrett-Joyner-Helenda (BJH) method, employing Kruk–Jaroniec–Sayari (KJS) equations on the adsorption branch of nitrogen isotherms.

Elemental analysis was used to determine the nitrogen content and corresponding amine loading of the materials. The C, H, N, S content was determined using a Thermo Electron Corporation CHNS-O analyzer.

SS NMR spectra were acquired on a Bruker Advance III 500 spectrometer and a wide bore 11.7 Tesla magnet with operational frequencies for ^{1}H, ^{29}Si and ^{13}C of 500.13, 99.35 and 125.77 MHz, respectively. A 4 mm triple resonance probe with MAS was employed in all the experiments. The samples were packed on a Zirconia rotor and spun at a MAS rate between 10 and 15 kHz. The magnitude of radio frequency (RF) fields, υ_{rf}, were 100 and 42 kHz for ^{1}H and ^{29}Si, respectively. The relaxation delays, d1, between accumulations were between 3 and 120s for ^{1}H and ^{29}Si MAS NMR, respectively. For the $^{13}C/^{1}H$ Cross Polarization (CP) MAS experiments, the RF fields υ_{rf}^{H} of 55 and 28 kHz were used for initial excitation and decoupling, respectively. During the CP period the ^{1}H RF field υ_{rf}^{H} was ramped using 100 increments, whereas the ^{13}C RF field υ_{rf}^{C} was maintained at a constant level. During the acquisition, the protons are decoupled from the carbons by using a two-pulse phase-modulated (TPPM) decoupling scheme. A moderate ramped RF field υ_{rf}^{H} of 62 kHz was used for spin locking, while the carbon RF field υ_{rf}^{C} was matched to obtain optimal signal and the CP contact time of 2ms were used. All chemical shifts are reported using δ scale and are externally referenced to tetramethylsilane (TMS) at 0 ppm.

Rotor synchronized spin echo sequence ($\pi/2 - \tau - \pi - \tau$ - acqu) was also applied to record the ^{1}H NMR spectra with τ delay time of 2010 μs. The delay time was chosen as an optimised compromise between the signal decay owing to relaxation and the resolution gain owing to longer delay times.

Dehydration was carried out directly on powder samples packed inside the NMR spinner, which was introduced in a special hand-made quartz cell connected to a high vacuum line (residual pressure 10^{-4} mbar) allowing both *in-situ* heat treatment (120 °C for 2h) and adsorption experiments. Then the spinner was extracted from the cell, rapidly closed and submitted to SS NMR analysis. Similarly, rehydration experiments were made *in-situ* (at water vapour pressure of 20 mbar for 30min) and allowed to equilibrate prior to SS NMR data recording.

Acidification of NH_2-MSN sample was carried out by soaking 100 mg of sample in 100 ml of a 0.001 N HCl solution (pH = 3) with 0.02 N KCl. The sample was left under magnetic stirring for 4 hours at room temperature, separated by centrifugation and dried in vacuum oven at 313 K for 4 h. Fourier Transform infrared (FTIR) spectra were recorded using a Vertex70 spectrometer (Bruker Optics) equipped with a DTGS detector, working with a resolution of 4 cm^{-1} over 64 scans. The spectra were obtained in transmission mode, with the samples pressed in the form of self-supporting pellets (*ca* 5.5 mg/cm^2) mechanically protected with a pure gold frame. Samples were placed in quartz cells equipped with KBr windows, allowing in situ activation, measurements and vapour dosage. Before the measurements the samples were outgassed at RT for 2 hours to remove adsorbed water and impurities. H_2O adsorption experiments were carried out by step-wise increase (maximum pressure of reported spectra 9 mbar) and subsequent decrease of water vapour equilibrium pressure until high vacuum.

Theoretical calculations have been performed at the Density Functional Theory (DFT) level, with hybrid functional B3LYP,[53-55] using Dunning's correlation-consistent cc-PVDZ basis set on light atoms,[56, 57] and LANL2DZ effective core potentials and basis set for silicon.[58] The contribution from dispersion (van der Waals) forces, often very important to determine the structures and the

relative energies of molecule/surface interfaces, was added through the atom-atom pairwise algorithm proposed by Grimme.[59]

A cluster model, with stoichiometry $Si_{52}O_{152}H_{93}$ was extracted from the MCM-41 structure, to simulate a region of the inner surface: hydrogen atoms were added to saturate the oxygen valences at the cluster border. On top of this cluster an aminopropylsilane molecule, $Si(OH)_3(CH_2)_3NH_2$, was grafted, by condensation of two or three Si-O-Si bonds as described below.

3. Results and discussion:

3.1 General properties

The pristine MSN and NH_2-MSN samples were characterized about their general properties, including textural and morphological features. The samples are composed by spheroidal nanoparticles (particle size 141 ± 44 nm) with a regular array of channels, as seen in HRTEM images (Figure 1). The mesostructure shows the hexagonal symmetry typical of the MCM-41 system, as also testified by XRD results, displaying the expected (100), (110), (200) and (210) peaks related to the P6mm symmetry group (Figure S1). In NH_2-MSN these peaks are slightly weaker and shifted in position with respect to the parent material, in that the d_{100} parameter moves from 37.7 to 37.2 Å (Table 1).

The nitrogen adsorption/desorption isotherms of both NH_2-MSN and parent material can be classified as type IV, typical of mesoporous materials (Figure S2). The measured SSA, pore volume and size are smaller in the functionalized NH_2-MSN material with respect to pristine MSN. On the contrary the wall thickness (calculated by combining d_{100} with the pore diameter, 4th and 5th columns of Table 1) increases from 8.6 to 13.0 Å. All these data are in agreement with what usually observed on post-synthesis functionalized mesoporous materials, suggesting the lining of the silica pores with the grafting agents, while preserving the ordered mesostructure. However, we have to be aware that a homogenous distribution of the grafting agents along the whole length of the channels is unlikely, due to diffusion problems and to the high reactivity of the APTS reactant. This might result in a higher concentration of aminopropyl groups at the pore entrances.[60]

^{29}Si distribution was investigated by ^{29}Si MAS NMR. Figure 2a shows the ^{29}Si MAS NMR spectra of pristine MSN sample, where Q^2, Q^3 and Q^4 sites are present. There is only one Q^4 (**Si**$(OSi)_4$) silicon sites at -111 ppm, with Q^3(**Si**$(OSi)_3OH$) sites at -102 ppm and Q^2 (**Si**$(OSi)_2(OH)_2$) sites at -92 ppm, each seen in MSN sample. As far as NH_2-MSN (Figure 2b) is concerned, besides the Q sites (Q^4 at -110, Q^3 at -101 and Q^2 at -92 ppm), T silicon sites [T^3 (R**Si**$(OSi)_3$) at -67 ppm, T^2 (R**Si**$(OSi)_2OH$) at -60 ppm] are also present, R being aminopropyl species.[61, 62] Relative concentrations of T^n and Q^n species obtained from ^{29}Si MAS NMR spectra are given in Table S1. Surface coverage (SC) of the mesopores with organic moieties were estimated according to SC = $(T^3 + T^2)/(Q^3 + Q^2 + T^3 + T^2)$ and found to be comparable with the values reported in the literature for similar materials.[61] Namely, Huh *et al*. reported a surface coverage value of 29 for aminopropyl functionalized mesoporous silica materials with MCM-41-type structure which is comparable with our sample's value 27. Szajna-Fuller *et al*. found a relative concentration of T-sites in their organic-MSN samples as 14 % which is comparable with our NH_2-MSN's value 13 %.[63] An increase in the relative intensity of Q^2 is observed on NH_2-MSN with respect to pristine material. This can be explained by the amine-assisted partial hydrolysis of siloxane bonds, as observed by Etienne et al.[64]

The grafting density of the functionalized material, as determined by elemental analysis of nitrogen was found to be 0.73 aminoproyl groups/nm^2. This value is in good agreement with the estimation of 0.90 groups/nm^2 obtained by thermogravimetric analysis (TGA, see Figure S3 and SI for further details). TGA was also carried out on the pristine MSN sample, to estimate the OH surface density by the weight loss between 150 and 1000 °C, which can be assigned to surface dehydroxylation (see SI). The calculated value of 3.3 OH/nm^2 (5.4 wt%) is lower with respect to the well-known one of about 4.5 OH/nm^2 (Kiselev–Zhuravlev constant)[65] and to what reported by many authors on mesoporous silica materials with similar infrared features (4.4-4.6 OH/nm^2, see below).[66, 67] On the other hand, relatively low values were determined by thermogravimetric analysis on MCM-41-like materials, see for instance Ishikawa et al. (3.3 OH/nm^2) and Llewellyn

et al. (1.2 OH/nm^2).[68, 69] Indeed, the difficulties related to an accurate calculation of surface OH density have been discussed by many authors, and often explained in relation to Si-OH accessibility.[66, 70] Notwithstanding the uncertainty about OH surface density (which is outside the scope of this work), we can be confident about the reported grafting density, in relation to the higher accuracy of the employed N elemental analysis.

The residual OH density of NH_2-MSN, calculated by TGA as described in SI, was found to be around 1.78 OH/nm^2, which could be an underestimated value, as discussed above. This is however in agreement with the fact that the process of functionalization is not complete, in that not all the surface silanol groups were consumed in the reaction (as confirmed by infrared evidences, see below). It is useful at this purpose to recall the fact that each 3-aminopropyl triethoxysilane molecule could react with two or three Si-OH groups, giving bi- or tri-legged grafted aminopropyl groups, as depicted in Scheme 1

3.2 Hydration dynamics in MSN

Figure 3(a-b) shows ^{1}H MAS NMR spectra of pristine and dehydrated MSN recorded at a MAS spin rate of 15 kHz. Only one peak at 4.6 ppm is present in the former and is due to weakly adsorbed water.[71, 72] At least three resonances are visible in the dehydrated sample with two being very broad components and one narrower contribution. Firstly, the sharp and intense band at 1.8 ppm is attributed to isolated silanols and the broad shoulder at 2-5 ppm to hydrogen bonded ones (Scheme 2). Further down-field, a very broad and weak peak in the range 4-8 ppm is also visible and is attributed to hydrogen bonded protons from silanols and/or hydrogen bonded water.[71, 72] This would suggest the presence, even after dehydration, of very small amounts of adsorbed water molecules. The breadth of the signal spanning 4 to 8 ppm can be ascribed to heterogeneous broadening associated with a wide distribution of chemical shifts provided by a large variety of hydrogen-bonds. This point will be discussed in detail in the following.

Comparison between dehydrated and hydrated MSN samples was also investigated by infrared spectroscopy, which is a powerful and proven technique to study the distribution of Si-OH surface groups and their interaction with probe molecules, including water. The obtained results (Figure S4) are similar to those already reported in the literature, and will not be described in detail in this work. We only acknowledge the fact that the spectral shape of dehydrated MSN, which is informative about the Si-OH concentration and distribution,[73] is similar to what reported by Gallas et al. and by Cauvel et al. for "bulk" (that is not nanosized) mesoporous silica.[66, 67] Both authors proposed for these materials an OH surface density of 4.4-4.6 OH/nm^2, in fair agreement with our TGA measurements (see above).

3.3 Hydration dynamics in NH_2-MSN.

The interaction of water with NH_2-MSN was followed by infrared spectroscopy, ^{1}H, ^{13}C and ^{29}Si MAS NMR. For sake of clarity infrared spectroscopy will be discussed first, followed by the SS NMR results.

3.3.1 Infrared spectroscopy.

The infrared spectrum of NH_2-MSN after outgassing at RT is reported in Fig. 4 as black curve. At high energy (top panel) one weak band is found at 3734 cm^{-1}, with a broad absorption between 3700 and 2500 cm^{-1} and clear components at 3370, 3306, 2940 and 2870 cm^{-1}. Among these, the bands at 3370 and 3306 cm^{-1} can be assigned to antisymmetric and symmetric NH_2 stretching modes (ν_{as} and ν_{sym}), while those at 2940 and 2870 cm^{-1} are clearly the ν_{as} and ν_{sym} CH_2 modes, confirming surface functionalization with aminopropyl groups.[52]

The weak band at 3734 cm^{-1} is related to residual Si-OH. Its position is lower with respect to isolated silanols (3744 cm^{-1}, Scheme 1a and dashed grey curve in Figure 4, top panel), so that it can be explained either as vicinal (*i.e.* H-bonding acceptor) or geminal Si-OH groups (Schemes 2b and 2c, respectively).[66] The broad absorption between 3700 and 2500 cm^{-1} testifies to the presence of H-

bonding interactions between surface groups. This is more intense and much broader with respect to what observed on dehydrated silica (dashed grey curve in Figure 4, top panel), suggesting an important role of the aminopropyl groups in H-bonding surface interactions, as discussed below.

The corresponding spectrum of dehydrated NH_2-MSN in the low frequency (black curve in Fig. 4, bottom panel) is dominated by a band at 1595 cm^{-1}, assigned to the δNH_2 scissor vibration. It is interesting to compare this typical vibration of grafted aminopropyl groups with that of amino groups in the gas phase, *i.e.* not hydrogen-bonding interacting. For instance, the gas phase spectrum of methylamine shows the δNH_2 band at 1620 cm^{-1},[74] and the same position was reported for aniline, where the presence of two components was proposed.[75] It is well known that the bending modes of A-H groups (A = O, N, etc.) are shifted to higher wavenumbers as a result of hydrogen bonding, at variance with the typical red-shift of the corresponding stretching modes.[76] An opposite trend is expected in the presence of H-bonding involving the nitrogen atom of the -NH_2 group as H-acceptor. The relatively low position of the δNH_2 band measured in this work thus suggests the predominance of –NH_2 groups acting as H-acceptors from Si-OH moieties. On these basis, pairs of interacting -NH_2 groups, where -NH_2 species also acts as H-donors, are thus unlikely to be present (or in negligible amount).

Coming back to the spectra reported in Figure 4, at the upper and lower sides of the band at 1595 cm^{-1} two broad absorptions are found at 1636 and 1550 cm^{-1}, which were assigned to the δ_{as} modes of protonated NH_3^+ species,[52, 76, 77] while the weak component at 1470-1475 cm^{-1} can be explained as the overlapping of δCH_2 and weak NH_3^+ δ_{sym} modes.[76] These features suggest an acid–base equilibrium between some amino groups and surface Si-OH, in agreement with what proposed in the literature on the basis of titration experiments.[39]

When water vapour is dosed on the NH_2-MSN sample, the main effect in the high energy bands (Figure 4 top panel, grey curves) is the increase of the broad absorption centred around 3200 cm^{-1}, testifying of H-bonding interactions of surface groups (both Si-OH and aminopropyl) with water

molecules. Noticeably, the band of residual Si-OH at 3734 cm^{-1} is almost totally consumed, leaving a very weak band at 3744 cm^{-1} due to less reactive isolated Si-OH.[66] The νNH_2 and νCH_2 modes of the functionalizing moieties are still observed at relatively high water dosage, even if they become broader and less resolved.

More information about the interactions taking place with water at the organic/inorganic silica surface can be obtained by the analysis of the low frequency range spectra (Fig. 4 bottom panel, grey curves). Upon water adsorption/desorption the 1595 cm^{-1} δNH_2 band is partially consumed, but it is still present at high water dosage. However, water dosage causes the increase of the two broad and intense bands at 1636 and 1550 cm^{-1}, with a weaker one at 1473 cm^{-1}. The assignment of these spectral features was not straightforward, due to the overlapping in the high frequency side of the typical δOH mode of adsorbed water (1630 cm^{-1}, see Figure S4). However, bands in similar position are expected in the presence of protonated NH_3^+ groups,[76] and were indeed observed for *n*-buthylammonium (*n*BA) ions embedded in microporous Si-doped aluminophosphate (SAPO) materials and stabilized by the negatively charged SAPO framework.[77]

This transformation was found to be reversible, in that the band at 1595 cm^{-1} was completely restored by decreasing water coverage (RT outgassing). To clarify this point an additional experiment was carried out on a NH_2-MSN sample subjected to an acidic treatment with an HCl/KCl solution (see experimental) and subsequently dehydrated. The resulting spectrum is reported in Figure 4 (bottom panel) as dotted curve. Two broad bands with maxima at 1612 and 1518 cm^{-1}, with an evident shoulder at 1595 cm^{-1}, characterize the curve. The latter is clearly related to the δNH_2 mode of aminopropyl groups, similarly to what discussed above. The former couple could instead be assigned to the two δ_{as} modes of protonated NH_3^+ species, also responsible for the sharp and weak peak at 1473 cm^{-1} (δ_{sym}). These results are in good agreement with what reported by Calvo et al., who deeply discussed the amino-ammonium speciation in similar materials.[28] The different position of these modes with respect to what observed on hydrated NH_2-MSN could be related to the different

counterions stabilizing the charged amine: hydroxide *vs* chloride. The protonated NH_3^+ groups were in fact not observed on the dehydrated NH_2-MSN material when the acidic treatment was carried out at the same pH without an excess of KCl. Moreover, the effect of the local environment on the vibrational properties of *n*BA was reported by Gieck et al. showing bands at 1612 and 1502 cm^{-1} in the CAL-1 SAPO material and at 1634 and 1555 cm^{-1} for the same ions intercalated between the layer of lamellar AlPO-ntu material.[77]

As a final comment, we underline the fact that not all the surface aminopropyl groups were involved in the interaction with water or were protonated after HCl/KCl treatment, as testified by the persistence of the component at 1595 cm^{-1} in both experiments (Figure 4, highest water coverage and dotted spectra, respectively). This is in agreement with the observations by Calvo et al., suggesting that a large fraction of aminopropyl groups in post-synthesis functionalized materials are not accessible.[78]

3.3.2 ^{1}H MAS NMR

The ^{1}H MAS NMR spectrum of pristine NH_2-MSN recorded at a MAS rate of 15 kHz is reported in Figure 3c. The proton spectrum mainly consists of contributions from adsorbed water and aminopropyl groups. The relatively narrow bands at 1.0 and 3.5 ppm are due to the methyl (C5) and methylene (C4) protons from unhydrolyzed ethoxy groups, which were not detected by infrared spectroscopy due to overlapping with the νCH_2 of the aminopropyl chain. In addition, peak at 0.85 ppm belongs to the methylene (C1) protons close to the silicon atom from the aminopropyl chains. The remaining CH_2 protons appear at 1.25 and 2.8 ppm, respectively, for middle (C2) and NH_2 bound (C3) groups.[79] The appearance of weak resonance at 1.95 ppm represents weakly interacting Si-OH groups, in agreement with infrared. The relatively broad and intense peak at 5.7 ppm is tentatively assigned to weakly physisorbed water. However, NH_2 protons also resonate around this chemical shift in a hydrated system and are clearly undistinguishable. Here, we have to recall that in pristine MSN sample, weakly adsorbed water resonate at 4.5 ppm. Therefore, 5.7 ppm peak in pristine NH_2-

MSN have also contributions from protonated-amine species (as evidenced by infrared spectroscopy) as well as hydrogen bonded silanols and water. However, protons of water molecules rapidly exchange with protons of NH_3^+ species and are difficult to distinguish in the ^1H MAS NMR spectrum. Figure 3d displays ^1H MAS spectrum of dehydrated (120 °C for 2 h in vacuum) NH_2-MSN sample. Dehydration treatment essentially broadened resonances due to methyl and methylene protons, especially the ones at 1.0 and 3.5 ppm. However, peak at 0.85 ppm attributed to C1 protons close to Si and at 1.25 ppm due to C2 protons remained more or less intact after dehydration. In addition, resonances assigned to weakly interacting Si-OH protons shifted from 1.95 to 1.6 ppm as well as C3 methylene protons moved from 2.8 to 2.5 ppm. The anisotropic broadening as well as the shift are consistent with a distribution of rigid environments for the aminopropyl groups and thus with a restricted mobility of the chains. It can be concluded that amino propyl species are principally in free form (not in Brönsted protonated state) in the dehydrated sample (Scheme 1) while both protonated and free forms co-exist in the pristine NH_2-MSN sample, in agreement with infrared evidences.

However in free form, NH_2 can exhibit extended hydrogen bonding architectures with residual Si-OH (see below the discussion of the theoretical modelling) and chemical shift values vary from a true free state. Interestingly, a broad component in the range 3-10 ppm is still present in the spectrum of dehydrated NH_2-MSN sample (Figure 3d). The above finding is consistent with infrared evidences and with the observations on hydrated MSN sample, with the broad peak representing strongly hydrogen bonded silanols, water and/or NH_2 species in widely distributed bonding environments in the pore surfaces. However, the high intensity as well as the broadness of this resonance (compared to MSN sample) in dehydrated NH_2-MSN sample suggests the participation of aminopropyl chains in hydrogen bonding with silanols and/or residual water.

Water removed by dehydration treatment was re-adsorbed by subsequent exposure to water vapour (20 mbar for 30 min) and the spectra in Figure S5 (a and c) are essentially the same suggesting that the water adsorption process and pore-filling mechanism are reversible.

Generally, protonated amine group resonate around 7 ppm, however, in NH_2-MSN sample this signal was difficult to resolve, partially due to proton background signal of the probe and partially due to strongly dipolar coupled proton spins (*e.g*. water). To suppress such effects, rotor synchronized spin echo pulse sequence was employed with a delay time of 2.01 ms. The echo spectra in Figure S6 exhibit a far superior baseline, where the lines of the relevant protons are nicely resolved. In Figure S6, the rotor synchronized echo MAS spectra are shown as a function of hydration level. The zoomed spectrum of pristine NH_2-MSN (Figure S6a') clearly exhibits a broad resonance at 6.9 ppm due to NH_3^+ species. Upon dehydration (Figure S6b') and subsequent rehydration (Figure S6c'), the peak intensity and line width remained similar, implying that a fraction of amine group is permanently protonated, in agreement with infrared data (see above). In addition, narrow resonance peaks are observed at 4.6, 5.0 and 5.3 ppm in the pristine as well as rehydrated sample. The absence of such resonances in the dehydrated sample shows that they are indeed due to water molecules and/or clusters interacting with surface site such as silanols and/or aminopropyl groups.

Finally, to further corroborate the data about reversible protonation of aminopropyl groups in the presence of water, solid state ^{1}H MAS NMR spectra were recorded on acidified NH_2-MSN sample as shown in Figure 3e and 3f. In hydrated state, physisorbed water, hydrogen bonded silanols and NH_3^+ species resonate as an intense peak at 5.3 ppm. However, in dehydrated state, isolated silanols and NH_3^+ species resonate at 1.6 and 7.0 ppm, respectively. It is important to note that, unhydrolysed ethoxy groups (C4 and C5 protons) are not visible in this sample as they have undergone hydrolysis during the acidification of sample.

3.3.2 ^{13}C CPMAS NMR

Standard CPMAS conditions were used to acquire the ^{13}C CPMAS NMR spectra of NH_2-MSN sample at room temperature in order to confirm the surface functionalization as well as to discriminate ^{13}C sites based on their mobility and to gather information concerning the protonation of the amino group.[61, 62] Figure 5a displays ^{13}C CPMAS spectrum of pristine NH_2-MSN sample with well-defined

signals at 8.7 and 42.2 ppm for carbon atoms C1 and C3, respectively. However, multiple resonances at 21.4, 24.5 and 29.6 ppm are visible for the central carbon (C2) atom of the propyl group.[80] In addition, broad resonances although less intense, centred at 59 and 16 ppm are also visible in the spectrum and are due to C4 and C5 carbons of the unreacted ethoxy group. These bands are more clearly discernible on the spectrum of the dehydrated sample (Figure 5b). The appearance of multiple resonances in ^{13}C CPMAS for identical central C2 carbon confirms the different environment experienced by the aminopropyl species. Since the chemical shift of the C2 carbon (two bonds from the nitrogen) is known to be very sensitive to the electronic environment of nitrogen in an aliphatic amine,[81] C2 chemical shift patterns is interpreted here in terms of structural changes occurring in the amino group. Pristine NH_2-MSN sample has high amount of physisorbed water and amino groups are either in free or protonated state and interacting predominantly with water molecules.

According to earlier reports, C2 carbon in free and protonated aminopropyl group resonate at *ca.* 28 and 21 ppm, respectively.[82] A partial positive charge may be present in amino group due to hydrogen bonding and in that particular case C2 carbon would resonate between the chemical shift values 21 and 28 ppm. Strictly speaking, NH_2 groups can be in a true free state or they can interact non-covalently with water molecules and SiOH groups. However, the variations in chemical shift of C2 carbon according to sample's hydration/dehydration state points towards the water dependent interactions associated with NH_2 groups. Water promoted changes in the non-covalent interactions of aminopropyl groups at the surface can be envisaged according to the equilibrium (1).[81] The elimination of water from the pristine sample would shift the equilibrium to hydrogen bonded amine state in the right. The amino groups are not merely bound by the amine-silanol hydrogen bonding but can be protonated in the presence of adsorbed water. This could be the result of proton transfer from silanols, or from water molecules.[32] In the former case, the effect of water would be to stabilize NH_3^+/OH^- couple through solvation. This aspect has been investigated by theoretical calculations (see below). The addition of water shifts the equilibrium to the hydrated ionic complex. In addition to the

above discussed states, a partially charged weakly interacting state may also co-exist in the NH_2-MSN sample.

$$-SiO^{-}(H_2O)_n\overset{+}{N}H_3-CH_2-CH_2-CH_2-Si \underset{+H_2O}{\overset{-H_2O}{\rightleftharpoons}} -SiOH\bullet\bullet\bullet\bullet NH_2-CH_2-CH_2-CH_2-Si-$$

(1)

Therefore, it can be concluded that, NH_2-MSN sample contains hydrogen bonded, protonated as well as weakly interacting aminopropyl species as evidenced by the resonance signals at 29.6, 21.4 and 24.5 ppm for C2 carbons (2", 2 and 2', respectively, in Figure 5a,b). Multifaceted cooperative interactions (electrostatic and non-covalent) between aminopropyl species and water as well as silanols can be envisaged in NH_2-MSN. The crucial role of adsorbed water in transfer of protons to amino groups as well as their hydrogen bonding capabilities are confirmed by the fact that identical spectra (to pristine NH_2-MSN) are obtained after rehydrating the dehydrated sample (data not shown). The rehydration experiments unveiled the transient effect of exposure to water.

In order to test the amine protonation hypothesis, we have recorded ^{13}C CPMAS NMR spectra on the acidified NH_2-MSN sample (pristine and dehydrated forms, Figures 5c and 5d, respectively. The weak signals at 59 and 16 ppm related to C4 and C5 carbon atoms (unhydrolysed ethoxy species) disappear, due to complete hydrolysis in acidic conditions. The major changes are observed on the relative intensity distribution of C2 carbons (2", 2 and 2' components). The pristine sample show a sharp resonance at 21.4 ppm and a minor signal at 29.6 ppm for C2 carbon, Figures 5c, which confirm the 100% Brönsted protonation due to treatment with HCl. While in the dehydrated sample, in addition to resonances at 21.4 ppm and 29.6 ppm, a broader resonance at 24.5 is also visible for the central carbon (C2) atom. This resonance distribution pattern for C2 carbon in dehydrated acidified sample is associated with mobility of aminopropyl chains.[81] As stated earlier, aminopropyl chain can co-exist in free-state or in non-covalently interacting state as shown in the scheme below. Earlier

theoretical/NMR studies have shown that the interaction between amine moieties and silanol groups on silica surface can strongly depend on the structure of the functional group.[40]

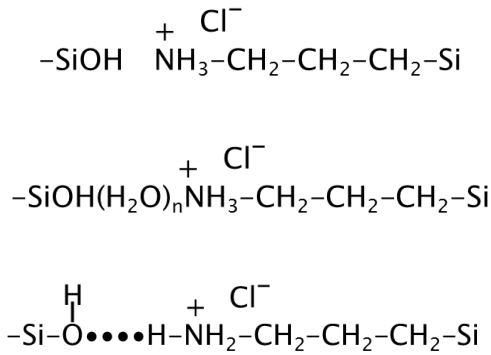

(2)

3.3.3 Theoretical calculations

The aminopropyl chain grafted on the silica surface was optimized in the cluster model described above, both with two and with three Si-O-Si bonds, the latter also in the presence of three water molecules. The number of water molecules employed for calculations was based on recent quantitative water adsorption measurements on the same sample,[44] indicating an average value of ca 3 water molecules per each aminopropyl group. All the optimized structures are illustrated in Figure 6, while the corresponding Cartesian coordinates are provided in the SI. In the bi-legged conformation, the aminopropyl chain sticks close to the surface, forming a rather strong hydrogen bond with a silanol group (O-N distance 2.68 Å), while in the tri-legged structure the greater rigidity of the organic/silica grafting keeps the amine chain perpendicular to the surface. However, when three water molecules are added to the tri-legged structure, the optimization leads to a large deformation of the organic/silica interface and the amine chain approaches the surface, establishing a hydrogen bond to a water molecule (O-N distance 2.67 Å), which is in turn H-bonded to a silanol group. The two other molecules form hydrogen bonds to the surface silanols, and weakly interact with the amine head too (see Figure 6d for detailed structure).

Thus the calculations confirm the presence of extended hydrogen bond networks in the hydrated samples: upon dehydration, it seems that only in the bi-legged conformation, with a residual ethoxy group, the amino group is able to bind to the surface silanols.

We also tried to simulate the formation of ammonium heads in the presence of water: however, all the calculations showed that the protonation of NH_2 is energetically unfavourable, even when the number of water molecules close to the organic chain is raised to five. On the other hand, the propylammonium ion in the tri-legged conformation resulted stable when the calculation was repeated adding a chloride anion, as shown in the SI (Fig. S7).

This result disagrees with the experimental findings, which indicate that ammonium ions actually form upon water vapour exposure to the surface of the aminopropyl/silica system: a possible reason is that water could be adsorbed preferentially close to pore entrance, resulting in higher concentration and better hydration of some organic chains. This is in agreement with the observation of Calvo *et al*. about the presence of a consistent fraction of not accessible aminoproyl groups.[78] Another possibility is that the local environment, thanks to the presence of the silanol networks, is more "solvating" than our limited model shows: in this case, water molecules and hydrogen bonded silanol groups could cooperate to make the ammonium formation possible.

Conclusions

Water confinement within the surface and nanoscale interior of functionalized mesoporous silica nanoparticles was studied using solid-state NMR and infrared spectroscopies. ^{1}H MAS NMR indicates a considerable range of water dynamics present in the unconditioned and dehydrated silica surface and interactions between aminopropyl species with water and silanols. ^{13}C CPMAS NMR gives insights on the bonding and protonation state of amine units. This picture was further supported by infrared spectroscopy, showing a complex network of hydrogen bonding interactions between silanols and amino groups in the dehydrated samples, together with unperturbed "free" amino groups and a small fraction of protonated ones. This situation was strongly perturbed by water adsorption,

causing the formation of a consistent fraction of protonated NH_3^+ groups, deriving from a reversible proton exchange mediated by the presence of water molecules.

The results were complemented by theoretical calculations at the DFT level, by considering two possible grafted aminopropyl groups, is the bi- and tri-legged ones. These showed a different conformation on the surface of silica, in that the former was found to be involved in hydrogen bonding with surface silanols, while this was not possible for the latter in relation to a greater rigidity. However, hydrogen bonding with the surface was favoured by the presence of water molecules. In contrast to NMR and infrared experimental evidences, calculations show that protonated aminopropyl groups are not stable in the presence of up to five water molecules, but can only be stabilized by the presence of a counterion such as Cl^-. Note that Calvo et al.[28] have shown with periodic DFT calculations based on plane waves that even with two water monolayers on the silica surface the protonated amino group is not stable and the proton is rapidly transferred to the silanolate moiety. We can thus hypothesize that the observed unusual reactivity of grafted aminoproyl groups in the presence of adsorbed water molecules could be related to specific circumstances not considered in the calculations, that is a high local density of water molecules (for instance at the pores entrance) and/or the presence of silanol networks solvating the NH_3^+ OH^- couples. The latter hypothesis is in agreement with the presence of a heterogeneous distribution of surface Si–OH group (patches of hydroxyl-rich regions alternating with hydroxyl-poor ones), as recently proposed for other mesoporous silica materials.[44, 67]

This study provides unprecedented detail on the surface features and reactivity of hybrid silica-based materials of wide employ, ranging from catalysis to biomedicine. The description of hydrogen bonding interactions and water dynamics could be of general interests for the researchers working in scientific fields where this class of materials finds applications, for a better understanding of their fate and properties.

Table 1 Textural and structural properties of the studied materials

Samples	SSA ($m^2 \cdot g^{-1}$)	Pore volume ($cm^3 \cdot g^{-1}$)	Pore diameter (Å)	d_{100} (Å)	Wall thickness (Å)
MSN	1090	1.35	35	37.7	8.6
NH_2-MSN	751	0.74	31	37.2	13.0

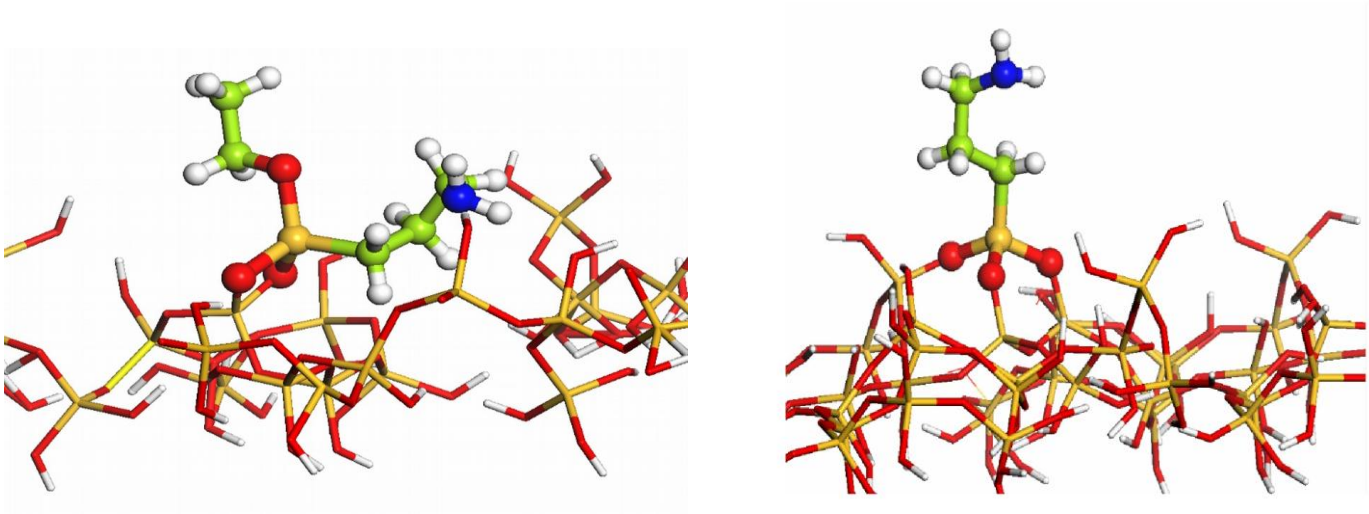

(a) (b)

Scheme 1. Cluster model of MCM-41 surface with aminopropyl grafted through two (a) or three (b) Si-O-Si bridges; in the bi-legged structure, an ethoxy group is still bound to the silane.

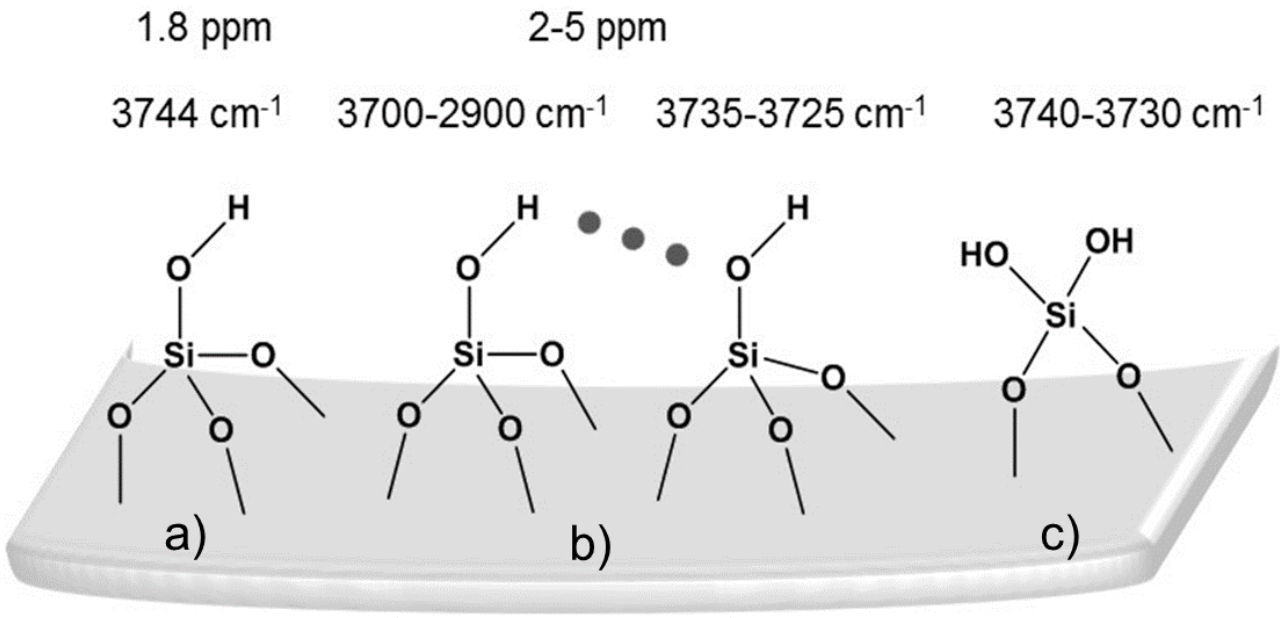

Scheme 2: Representative cartoon of the silanol groups mentioned in this work with corresponding infrared frequencies and NMR resonances: a) isolated, b) vicinal silanols with H- bonding interaction (donor and acceptor from left to right), c) geminal. The hydrogen bond is represented by a dotted line

Figure captions

Figure 1. Representative HRTEM images of a) pristine MSN and b) NH_2-MSN samples showing the spheroidal morphology and ordered mesoporous hexagonal structure.

Figure 2. ^{29}Si MAS NMR spectra of pristine MSN (a) and NH_2-MSN (b) samples at a MAS rate of 10 kHz. Each curve includes experimental and its deconvoluted spectrum with individual contribution from each ^{29}Si sites.

Figure 3.^{1}H solid state MAS-NMR spectra at a MAS rate of 15 kHz before (a, c, e) and after dehydration (b, d, f). a) and b) refers to pristine MSN, c) and d) to NH_2-MSN, e) and f) to acidified NH_2-MSN.

Figure 4. Infrared spectra in the high (top) and low (bottom) frequency ranges of NH_2-MSN initially contacted with 9 mbar of water vapour pressure at RT (light gray curve) and then progressively outgassed (gray curves) until high vacuum (black curve). Dashed grey curve in top panel refers to outgassed MSN for comparison. Dotted curve in bottom panel was obtained on acidified NH_2-MSN after prolonged outgassing.

Figure 5.^{13}C solid state CPMAS-NMR spectra of NH_2-MSN before (a) and after dehydration (b). c) and d) refer to the same experiment carried out on the acidified samples. A cross polarization contact time of 2 ms and a MAS rate of 10 kHz was used in all experiments.

Figure 6. Optimized structures of aminopropyl grafted on the MSN cluster model: (a) bi-legged structure, with a silanol group H-bonded to the amine head; (b) tri-legged structure; (c) tri-legged structure with three water molecules added; (d) detail of the hydrogen bond network in the tri-legged structure with water.

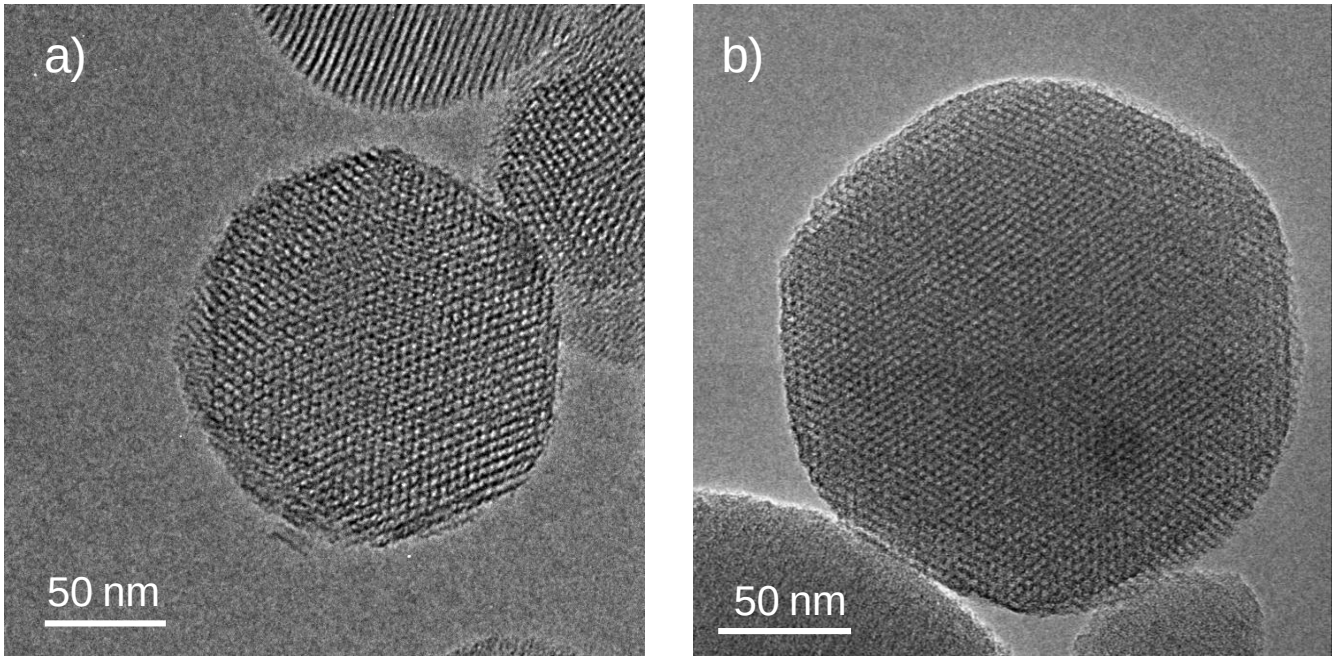

Figure 1

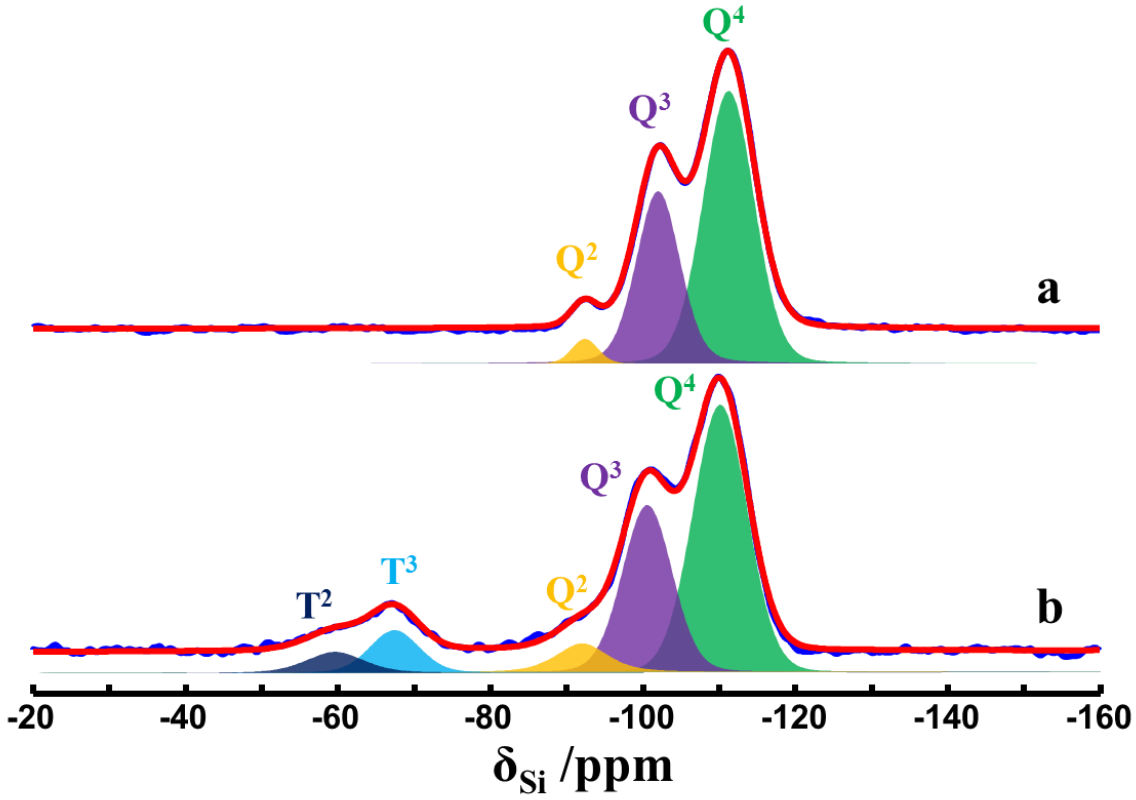

Figure 2

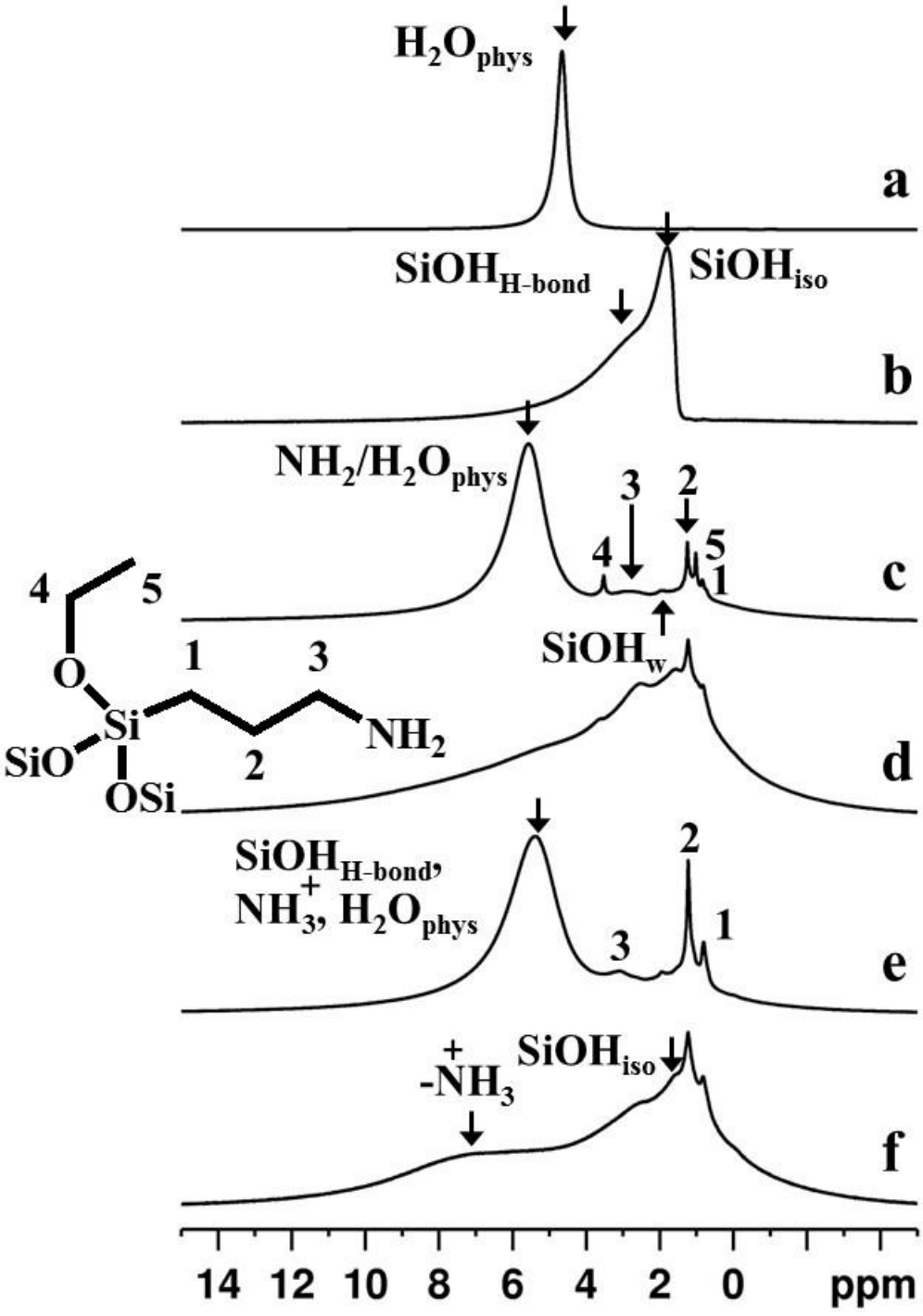
H2Ophys
a
SiOHH-bond
SiOHiso
b
NH2/H2Ophys
3
2
4
5
1
c
4
5
1
3
O
Si
SiO
2
NH2
OSi
SiOHw
d
SiOHH-bond,
NH3+, H2Ophys
2
3
1
e
-NH3+
SiOHiso
f
14 12 10 8 6 4 2 0 ppm

Figure 3

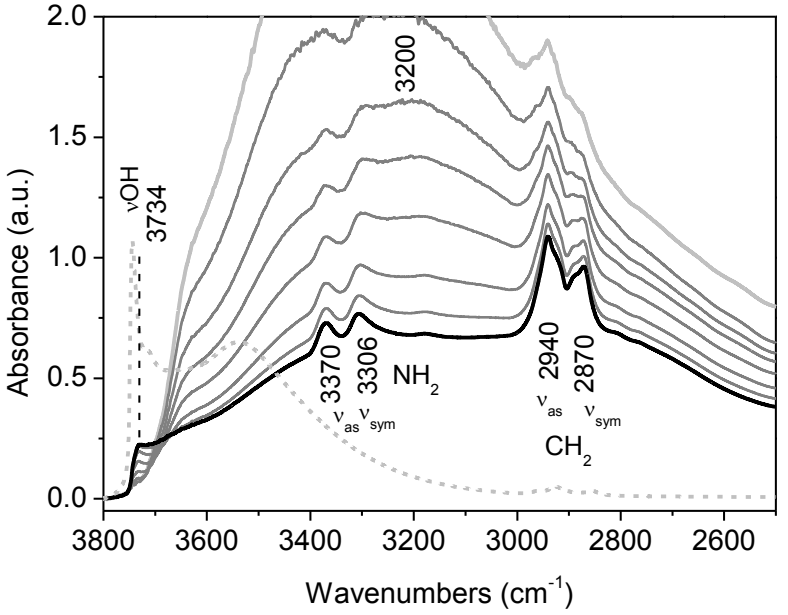
Absorbance (a.u.)
Wavenumbers (cm-1)
νOH
3734
3200
3370
3306
NH2
νas
νsym
2940
2870
CH2

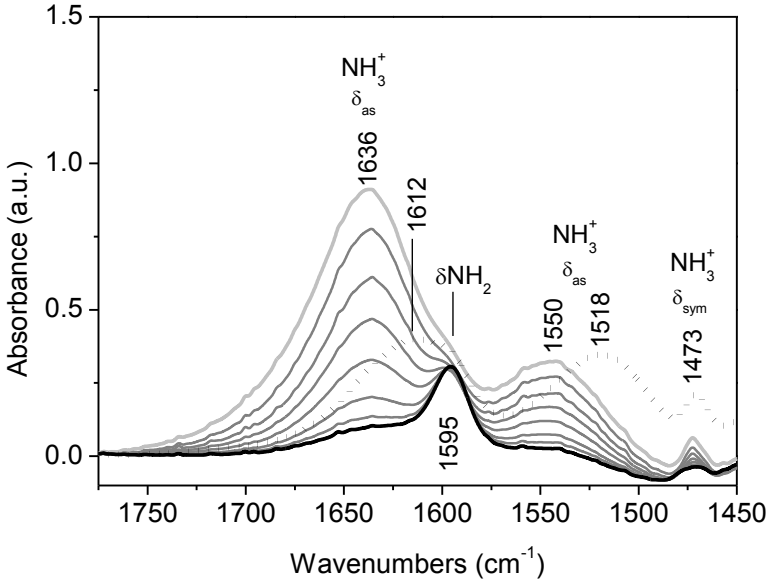
Absorbance (a.u.)
Wavenumbers (cm-1)
NH3+
δas
1636
1612
δNH2
1595
1550
1518
1473
NH3+
δsym

Figure 4

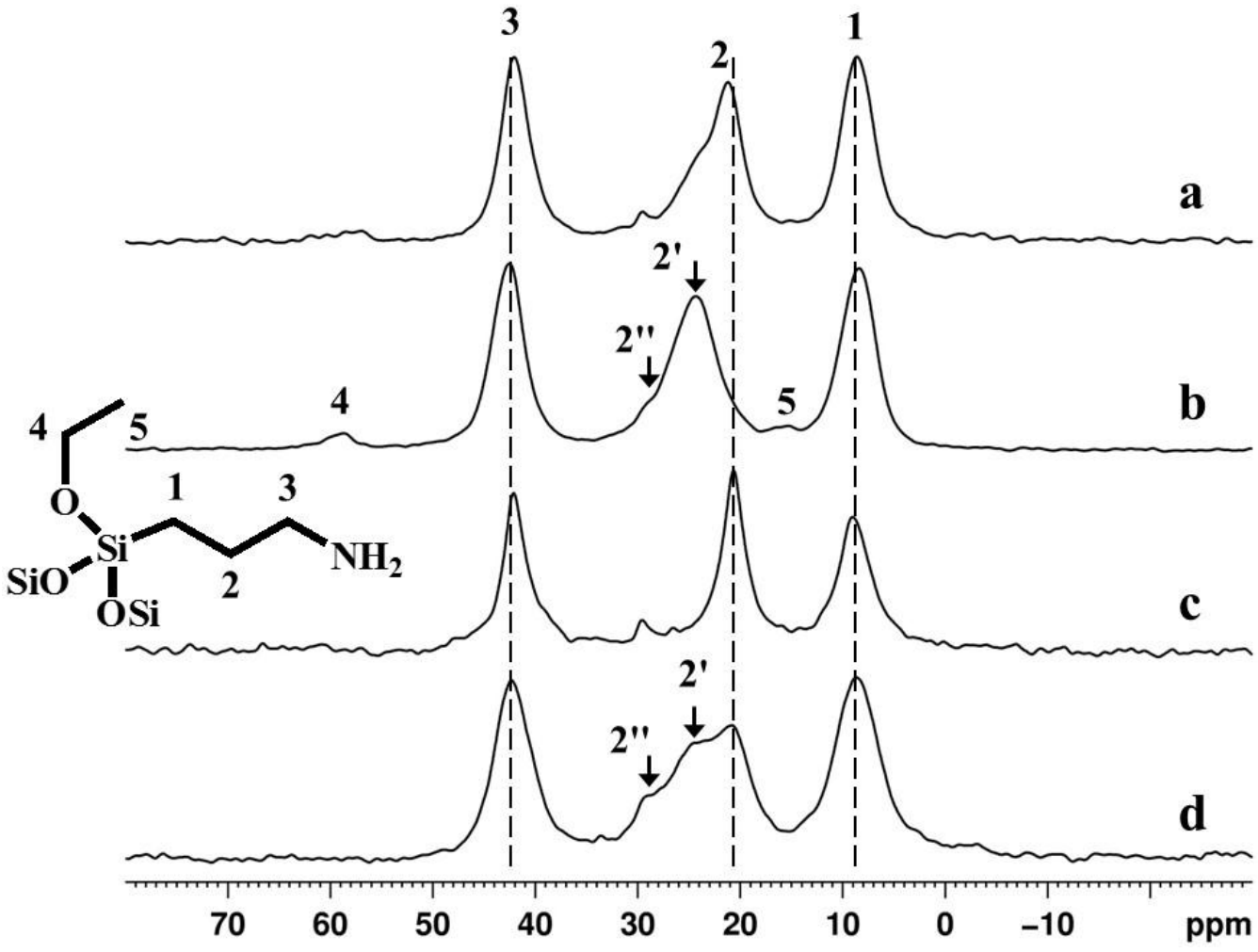
3
2
1
a
2'
2''
4
5
b
4
5
O
1
3
Si
NH2
SiO
2
OSi
c
2'
2''
d
70
60
50
40
30
20
10
0
−10
ppm

Figure 5

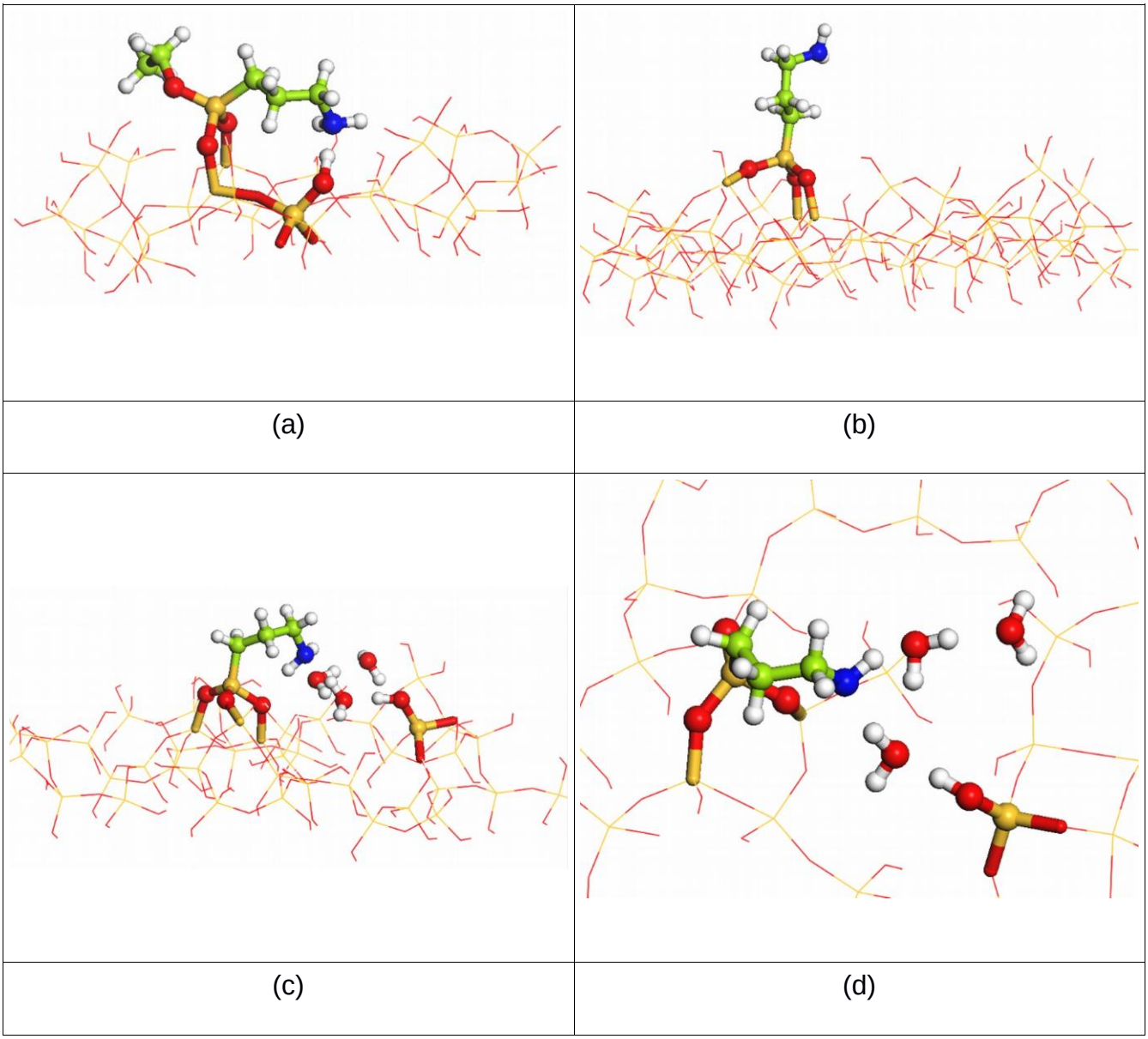

Figure 6

References

[1] M. Alvaro, B. Ferrer, V. Fornes, H. Garcia *ChemPhysChem*. **2003**, 4, 612-617.

[2] A. Domenech, M. Alvaro, B. Ferrer, H. Garcia *J. Phys. Chem. B.* **2003**, 107, 12781-12788.

[3] A. Walcarius, D. Mandler, J. A. Cox, M. Collinson, O. Lev *J. Mater. Chem.* **2005**, 15, 3663-3689.

[4] W. Li, R. Yuan, Y. Chai *Talanta*. **2010**, 82, 367-371.

[5] M. Luka, S. Karreman, S. Polarz *J. Mater. Chem. A.* **2015**, 3, 22017-22020.

[6] A. Corma, H. Garcia *Adv. Synth. Catal.* **2006**, 348, 1391-1412.

[7] U. Diaz, D. Brunel, A. Corma *Chem. Soc. Rev.* **2013**, 42, 4083-4097.

[8] B. Hatton, K. Landskron, W. Whitnall, D. Perovic, G. A. Ozin *Acc. Chem. Res.* **2005**, 38, 305-312.

[9] F. Hoffmann, M. Cornelius, J. Morell, M. Froba *Angew. Chem. Int. Ed.* **2006**, 45, 3216-3251

[10] Q. Yang, J. Liu, L. Zhang, C. Li *J. Mater. Chem.* **2009**, 19, 1945-1955.

[11] N. Brun, P. Hesemann, G. Laurent, C. Sanchez, M. Birot, H. Deleuze, R. Backov *New J. Chem.* **2013**, 37, 157-168.

[12] S. El Hankari, A. El Kadib, A. Finiels, A. Bouhaouss, J. J. E. Moreau, C. M. Crudden, D. Brunel, P. Hesemann *Chem. Euro J.* **2011**, 17, 8984-8994.

[13] B. Motos-Perez, J. Roeser, A. Thomas, P. Hesemann *Appl. Organomet. Chem.* **2013**, 27, 290-299.

[14] J. Gao, X. Zhang, Y. Yang, J. Ke, X. Li, Y. Zhang, F. Tan, J. Chen, X. Quan *Chem.-Asian J.* **2013**, 8, 934-938.

[15] M. Petrova, M. Guigue, L. Venault, P. Moisy, P. Hesemann *Phys. Chem. Chem. Phys.* **2015**, 17, 10182-10188.

[16] T. X. Bui, S.-Y. Kang, S.-H. Lee, H. Choi *J. Hazard. Mater.* **2011**, 193, 156-163.

[17] L. Vidal, O. Robin, J. Parshintsev, J.-P. Mikkola, M.-L. Riekkola *J. Chromatogr. A.* **2013**, 1285, 7-14.

[18] M. A. O. Lourenco, C. Siquet, M. Sardo, L. Mafra, J. Pires, M. Jorge, M. L. Pinto, P. Ferreira, J. R. B. Gomes *J. Phys. Chem. C*. **2016**, 120, 3863-3875.

[19] M. R. Mello, D. Phanon, G. Q. Silveira, P. L. Llewellyn, C. M. Ronconi *Microporous Mesoporous Mater.* **2011**, 143, 174-179.

[20] M. Vallet-Regí, F. Balas, D. Arcos *Angew. Chem. Int. Edit.* **2007**, 46, 7548-7558.

[21] J. M. Rosenholm, M. Linden *J. Control. Release*. **2008**, 128, 157-164.

[22] H. Meng, M. Xue, J. I. Zink, A. E. Nel *J. Phys. Chem. Lett.* **2012**, 3, 358-359.

[23] S. H. Wu, Y. S. Lin, Y. Hung, Y. H. Chou, Y. H. Hsu, C. Chang, C. Y. Mou *ChemBioChem*. **2008**, 9, 53-57.

[24] F. Porta, G. E. M. Lamers, J. Morrhayim, A. Chatzopoulou, M. Schaaf, H. den Dulk, C. Backendorf, J. I. Zink, A. Kros *Adv. Healthc. Mater.* **2013**, 2, 281-286.

[25] S.-H. Wu, Y. Hung, C.-Y. Mou *Chem. Commun.* **2011**, 47, 9972-9985.

[26] S. El Hankari, B. Motos-Perez, P. Hesemann, A. Bouhaouss, J. J. E. Moreau *Chem. Commun.* **2011**, 47, 6704-6706.

[27] J. Rosenholm, C. Sahlgren, M. Linden *J. Mater. Chem.* **2010**, 20, 2707-2713.

[28] A. Calvo, P. C. Angelome, V. M. Sanehez, D. A. Scherlis, F. J. Williams, G. J. A. A. Soler-Illia *Chem. Mater*. **2008**, 20, 4661-4668.

[29] J. P. Blitz, V. M. Gun'ko, R. Samala, B. A. Lawrence *Colloid Surf. A*. **2014**, 462, 1-8.

[30] M. Etienne, A. Walcarius *Talanta*. **2003**, 59, 1173-1188.

[31] S. E. Lehman, Y. Tataurova, P. S. Mueller, S. V. S. Mariappan, S. C. Larsen *J. Phys. Chem. C*. **2014**, 118, 29943-29951.

[32] A. A. Golub, A. I. Zubenko, B. V. Zhmud *J. Colloid Interface Sci.* **1996**, 179, 482-487.

[33] A. Walcarius, M. Etienne, B. Lebeau *Chem. Mater.* **2003**, 15, 2161-2173.

[34] C. H. Lee, S. H. Park, W. Chung, J. Y. Kim, S. H. Kim *Colloid Surf. A*. **2011**, 384, 318-322.

[35] K. C. Vrancken, L. Decoster, P. Vandervoort, P. J. Grobet, E. F. Vansant *J. Colloid Interface Sci.* **1995**, 170, 71-77.

[36] K. C. Vrancken, K. Possemiers, P. Vandervoort, E. F. Vansant *Colloid Surf. A*. **1995**, 98, 235-241.

[37] K. C. Vrancken, P. Vandervoort, I. Gillisdhamers, E. F. Vansant, P. Grobet *J. Chem. Soc., Faraday Trans.* **1992**, 88, 3197-3200.

[38] T. G. Waddell, D. E. Leyden, M. T. DeBello *J. Am. Chem. Soc.* **1981**, 103, 5303-5307.

[39] Y. Tataurova, M. J. Sealy, R. G. Larsen, S. C. Larsen *J. Phys. Chem. Lett.* **2012**, 3, 425-429.

[40] S. Nedd, T. Kobayashi, C.-H. Tsai, I. I. Slowing, M. Pruski, M. S. Gordon *J. Phys. Chem. C*. **2011**, 115, 16333-16339.

[41] M. Etienne, S. Goubert-Renaudin, Y. Rousselin, C. Marichal, F. Denat, B. Lebeau, A. Walcarius *Langmuir*. **2009**, 25, 3137-3145.

[42] J. M. Rosenholm, A. Duchanoy, M. Linden *Chem. Mater*. **2008**, 20, 1126-1133.

[43] J.-P. Dacquin, H. E. Cross, D. R. Brown, T. Duren, J. J. Williams, A. F. Lee, K. Wilson *Green Chem.* **2010**, 12, 1383-1391.

[44] G. E. Musso, E. Bottinelli, L. Celi, G. Magnacca, G. Berlier *Phys. Chem. Chem. Phys.* **2015**, 17, 13882-13894.

[45] S. T. Kim, K. Saha, C. Kim, V. M. Rotello *Acc. Chem. Res.* **2013**, 46, 681-691.

[46] A. Walcarius, M. Etienne, J. Bessiere *Chem. Mater*. **2002**, 14, 2757-2766.

[47] Q. Wang, E. Jordan, D. F. Shantz *J. Phys. Chem. C*. **2009**, 113, 18142-18151.

[48] M. A. Ramos, M. H. Gil, E. Schacht, G. Matthys, W. Mondelaers, M. M. Figueiredo *Powder Technol.* **1998**, 99, 79-85.

[49] D. Tarn, M. Xue, J. I. Zink *Inorg. Chem.* **2013**, 52, 2044-2049.

[50] D. R. Radu, C. Y. Lai, K. Jeftinija, E. W. Rowe, S. Jeftinija, V. S. Y. Lin *J. Am. Chem. Soc.* **2004**, 126, 13216-13217.

[51] K. M. Parida, D. Rath *J. Mol. Catal. A -Chem.* **2009**, 310, 93-100.

[52] P. Iliade, I. Miletto, S. Coluccia, G. Berlier *Res. Chem. Intermed.* **2012**, 38, 785-794.

[53] A. D. Becke *Phys. Rev. A: At., Mol., Opt. Phys.* **1988**, 38, 3098-3100.

[54] A. D. Becke *J. Chem. Phys.* **1993**, 98, 1372-1377.

[55] C. T. Lee, W. T. Yang, R. G. Parr *Phys. Rev. B.* **1988**, 37, 785-789.

[56] T. H. Dunning *J. Chem. Phys.* **1989**, 90, 1007-1023.

[57] R. A. Kendall, T. H. Dunning, R. J. Harrison *J. Chem. Phys.* **1992**, 96, 6796-6806.

[58] P. J. Hay, W. R. Wadt *J. Chem. Phys.* **1985**, 82, 270-283.

[59] T. Schwabe, S. Grimme *Phys. Chem. Chem. Phys.* **2006**, 8, 4398-4401.

[60] M. H. Lim, A. Stein *Chem. Mater.* **1999**, 11, 3285-3295.

[61] S. Huh, J. W. Wiench, J. C. Yoo, M. Pruski, V. S. Y. Lin *Chem. Mater.* **2003**, 15, 4247-4256.

[62] Z. H. Luan, J. A. Fournier, J. B. Wooten, D. E. Miser *Microporous Mesoporous Mater.* **2005**, 83, 150-158.

[63] E. Szajna-Fuller, Y. L. Huang, J. L. Rapp, G. Chaka, V. S. Y. Lin, M. Pruski, A. Bakac *Dalton Trans.* **2009**, 3237-3246.

[64] E. Seguin, S. Thomas, P. Bazin, G. Bond, C. Henriques, F. Thibault-Starzyk *Phys. Chem. Chem. Phys.* **2009**, 11, 1697-1701.

[65] L. T. Zhuravlev *Colloid Surf. A.* **2000**, 173, 1-38.

[66] J. P. Gallas, J. M. Goupil, A. Vimont, J. C. Lavalley, B. Gil, J. P. Gilson, O. Miserque *Langmuir*. **2009**, 25, 5825-5834.

[67] A. Cauvel, D. Brunel, F. DiRenzo, E. Garrone, B. Fubini *Langmuir*. **1997**, 13, 2773-2778.

[68] T. Ishikawa, M. Matsuda, A. Yasukawa, K. Kandori, S. Inagaki, T. Fukushima, S. Kondo *Journal of the Chemical Society-Faraday Transactions*. **1996**, 92, 1985-1989.

[69] P. L. Llewellyn, F. Schuth, Y. Grillet, F. Rouquerol, J. Rouquerol, K. K. Unger *Langmuir*. **1995**, 11, 574-577.

[70] X. S. Zhao, G. Q. Lu, A. K. Whittaker, G. J. Millar, H. Y. Zhu *J. Phys. Chem. B.* **1997**, 101, 6525-6531.

[71] B. Grunberg, T. Emmler, E. Gedat, I. Shenderovich, G. H. Findenegg, H. H. Limbach, G. Buntkowsky *Chem. Euro J.* **2004**, 10, 5689-5696.

[72] J. Trebosc, J. W. Wiench, S. Huh, V. S. Y. Lin, M. Pruski *J. Am. Chem. Soc.* **2005**, 127, 3057-3068.

[73] P. Ugliengo, M. Sodupe, F. Musso, I. J. Bush, R. Orlando, R. Dovesi *Adv. Mater.* **2008**, 20, 4579-4583.

[74] S. R. L. U. U.-E. Contract, Methylamine, NIST Standard Reference Data Program,74-89-5, **2009**.

[75] M. Mukherjee, B. Bandyopadhyay, P. Biswas, T. Chakraborty *Indian J. Phys*. **2012**, 86, 201-208.

[76] G. Socrates, Infrared and Raman characteristic group frequencies, John Wiley & Sons Ltd, Chichester, England, **2006**.

[77] C. Gieck, C. Bisio, L. Marchese, Y. Filinchuk, C. E. Da Silva, H. O. Pastore *Angew. Chem. Int. Edit.* **2007**, 46, 8895-8897.

[78] A. Calvo, M. Joselevich, G. Soler-Illia, F. J. Williams *Microporous Mesoporous Mater.* **2009**, 121, 67-72.

[79] J. J. Yang, I. M. ElNahhal, I. S. Chuang, G. E. Maciel *J. Non-Cryst. Solids*. **1997**, 209, 19-39.

[80] P. Innocenzi, Y. L. Zub, V. G. Kessler, Sol–gel methods for materials processing, Springer Science, Netherlands, **2008**.

[81] G. S. Caravajal, D. E. Leyden, G. R. Quinting, G. E. Maciel *Anal. Chem.* **1988**, 60, 1776-1786.

[82] X. G. Wang, K. S. K. Lin, J. C. C. Chan, S. F. Cheng *J. Phys. Chem. B.* **2005**, 109, 1763-1769.